

A Method to Predict Electromigration Failure of Metal Lines

著者	坂 真澄
journal or publication title	Journal of applied physics
volume	86
number	11
page range	6043-6051
year	1999
URL	http://hdl.handle.net/10097/35465

doi: 10.1063/1.371652

A method to predict electromigration failure of metal lines

Kazuhiko Sasagawa^{a)}

Department of Intelligent Machines and System Engineering, Hirosaki University, 3 Bunkyo-cho, Hirosaki 036-8561, Japan

Kazushi Naito and Masumi Saka

Department of Mechanical Engineering, Tohoku University, Aoba 01, Aramaki, Aoba-ku, Sendai 980-8579, Japan

Hiroiyuki Abé

Tohoku University, 2-1-1 Katahira, Aoba-ku, Sendai 980-8577, Japan

(Received 10 August 1998; accepted for publication 3 September 1999)

A new calculation method of atomic flux divergence (AFD_{gen}) due to electromigration has recently been proposed by considering all the factors on void formation, and AFD_{gen} has been identified as a parameter governing void formation by observing agreement of the numerical prediction of the void with experiment. In this article, a method to predict the electromigration failure of metal lines was proposed by using AFD_{gen}. Lifetime and failure site in a polycrystalline line were predicted by numerical simulation of the processes of void initiation, its growth to line failure, where the change in distributions of current density and temperature with void growth was taken into account. The usefulness of this prediction method was verified by the experiment where the angled aluminum line was treated. The failure location was determined by the line shape and the operating condition. The present simulation accurately predicted the lifetime as well as the failure location of the metal line.

© 1999 American Institute of Physics. [S0021-8979(99)08823-4]

I. INTRODUCTION

Electromigration is one of the key reasons of metal line failure with scaling down the packaged silicon integrated circuit. It is essential in the study of reliability of integrated circuit to predict the lifetime of the metal line. The lifetime under operating condition is predicted based on the results obtained from acceleration tests under high temperature and high input current density. For the extrapolation of the results to the operating condition the empirical Black's equation¹ is widely used.

The lifetime of the metal line is closely associated with void formation.² Divergence of the atomic flux by electromigration gives rise to the formation of void and the atomic flux divergence occurs at the triple point of grain boundary³ and grain boundary itself.⁴ Current density and temperature are effective factors on the atomic flux divergence at the triple point and, in addition to current density and temperature, their gradients are effective factors on that in the grain boundary.⁵ Since distributions of the factors in a metal line depend on testing conditions such as input current density and substrate temperature, the mechanism of void formation is varied by the testing condition even at the same point; that is the dominant mode of void formation is altered whether it is atomic flux divergence at the triple point or that at the grain boundary. Accordingly the distribution of void formation in the metal line is varied by the testing condition. In practice Lloyd, *et al.*⁶ reported that failure location changed with input current density.

Black's equation is given as

$$\tau = A j_{\text{in}}^{-n} \exp\left(\frac{Q}{kT}\right), \quad (1)$$

where τ is the lifetime, j_{in} is input current density, k is Boltzmann's constant, T is absolute temperature, n represents current density dependence and takes the value of 1–3,⁷ Q is activation energy which represents temperature dependence and takes the value of 0.4–0.8 eV, and A is a constant depending on film characteristic and line shape. The constants n , Q , and A are obtained based on mean-time-to-failure in the acceleration test. Adequateness of the extrapolation by Black's equation is doubtful because n is affected by choice of input current density in the acceleration test⁸ and the change in mechanism of void formation under the accelerated condition to that under the operating condition is not able to be taken into account. In the acceleration test with higher current density, n is evaluated to be more even in the same line.⁸ Under greater n the constant A is evaluated to be more. In the case of large n and A , the lifetime may be predicted longer than the true value through extrapolation by means of the substitution of much smaller current density in comparison with that in the acceleration test into j_{in} in Eq. (1). Furthermore, in the application of Black's equation to different line shape the acceleration tests to determine the constants for respective line shapes are required even if the film characteristic is the same.

Recently, Sasagawa *et al.*⁵ proposed a new calculation method of atomic flux divergence (AFD_{gen}) by considering all the factors on void formation, that is, current density, temperature, their gradients and film characteristics, and AFD_{gen} was identified as a parameter governing void formation by observing agreement of the numerical prediction of

^{a)}Electronic mail: sasagawa@cc.hirosaki-u.ac.jp

the void with experiment. In this study a method to predict electromigration failure of the metal line is proposed by using AFD_{gen} . Lifetime and failure site in a polycrystalline line are predicted by means of numerical simulation of the processes of void initiation, its growth to line failure using AFD_{gen} , where the change in distributions of current density and temperature with void growth is taken into account. The advantage of this method is to predict the failure based on a theory of void formation mechanism, not empirically, and to universally predict the failure by using only the film characteristic determined from the acceleration test, which is independent not only of test conditions but also of line shape. Accordingly this method would shorten a testing time for the prediction and provide a more accurate prediction. Finally, the usefulness of this prediction method is verified by experiment where an angled aluminum line is treated.

II. PREDICTION METHOD

A. Calculation method of AFD_{gen}

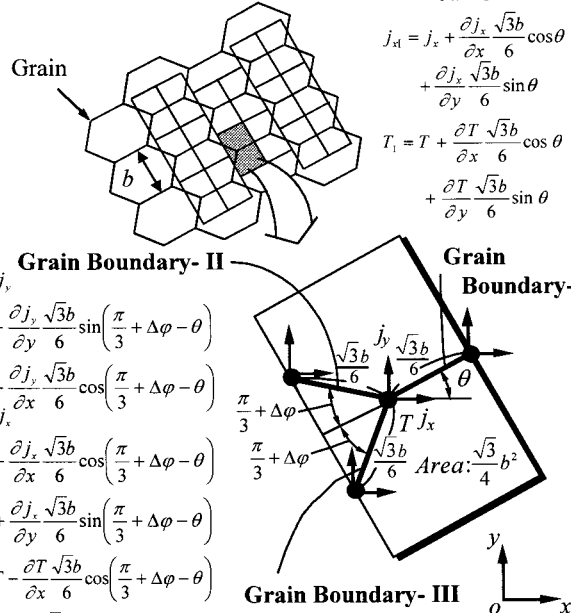
The governing parameter of electromigration damage AFD_{gen} has been proposed by Sasagawa *et al.*⁵ for both cases of polycrystalline line and bamboo line. Here summary of the calculation method of AFD_{gen} for the polycrystalline line is shown. The governing parameter AFD_{gen} for polycrystalline line is formulated based on the following considerations. The atomic transportation by electromigration is modeled by⁹

$$\mathbf{J} = \frac{ND_0}{kT} \exp\left(-\frac{Q_{gb}}{kT}\right) Z^* e \rho |\mathbf{j}| \cos \phi, \quad (2)$$

where \mathbf{J} is the atomic flux vector, N is the atomic density, D_0 is a prefactor, Q_{gb} is the activation energy for grain boundary, Z^* is the effective valence, e is electronic charge, \mathbf{j} is the current density vector, and ϕ is the angle between the current density vector and grain boundary. The temperature-dependent resistivity ρ is expressed as $\rho = \rho_0 \{1 + \alpha(T - T_s)\}$ where ρ_0 is the resistivity and α is the temperature coefficient at the substrate temperature T_s . A model of the grain boundary texture is shown in Fig. 1, where b is the average grain size, θ is the angle between grain boundary I and the x axis, and $\Delta\varphi$ is the minute angle which deviates from 120° on the angle between grain boundary II and III. The components of current density vector and temperature at the end of each grain boundary I, II, and III are shown in Fig. 1. From the components and temperature, the atomic flux along the grain boundary at the end of each grain boundary is obtained, and the change in number of atoms within a unit rectangular region per unit time is given. The number of atoms is divided by the volume of the unit region. Concerning the void formation, the atomic flux divergence AFD_{gen} is derived as

$$AFD_{gen} = \frac{1}{4\pi} \int_0^{2\pi} (AFD_{gb\theta} + |AFD_{gb\theta}|) d\theta, \quad (3)$$

where



$$j_{II} = j_y + \frac{\partial j_y \sqrt{3b}}{\partial y} \frac{\sqrt{3b}}{6} \sin\left(\frac{\pi}{3} + \Delta\varphi - \theta\right) - \frac{\partial j_y \sqrt{3b}}{\partial x} \frac{\sqrt{3b}}{6} \cos\left(\frac{\pi}{3} + \Delta\varphi - \theta\right)$$

$$T_{II} = T - \frac{\partial T \sqrt{3b}}{\partial x} \frac{\sqrt{3b}}{6} \cos\left(\frac{\pi}{3} + \Delta\varphi - \theta\right) + \frac{\partial T \sqrt{3b}}{\partial y} \frac{\sqrt{3b}}{6} \sin\left(\frac{\pi}{3} + \Delta\varphi - \theta\right)$$

$$j_{III} = j_x - \frac{\partial j_x \sqrt{3b}}{\partial x} \frac{\sqrt{3b}}{6} \cos\left(\frac{\pi}{3} + \Delta\varphi + \theta\right) - \frac{\partial j_x \sqrt{3b}}{\partial y} \frac{\sqrt{3b}}{6} \sin\left(\frac{\pi}{3} + \Delta\varphi + \theta\right)$$

$$T_{III} = T - \frac{\partial T \sqrt{3b}}{\partial x} \frac{\sqrt{3b}}{6} \cos\left(\frac{\pi}{3} + \Delta\varphi + \theta\right) - \frac{\partial T \sqrt{3b}}{\partial y} \frac{\sqrt{3b}}{6} \sin\left(\frac{\pi}{3} + \Delta\varphi + \theta\right)$$

FIG. 1. A model of the grain boundary texture of polycrystalline line structure introduced for formulation of AFD_{gen} . Constant b is the average grain size and the area of unit of the rectangular region, which contains only one triple point constituted by three grain boundaries having the length of $\sqrt{3}b/6$, is supposed to be $\sqrt{3}b^2/4$. The thickness of the unit region is assumed to be unity.

$$AFD_{gb\theta} = C_{gb} \rho \frac{4}{\sqrt{3}b^2} \frac{1}{T} \exp\left(-\frac{Q_{gb}}{kT}\right) \left[\sqrt{3} \Delta\varphi (j_x \cos \theta + j_y \sin \theta) - \frac{b}{2} \Delta\varphi \left(\left(\frac{\partial j_x}{\partial x} - \frac{\partial j_y}{\partial y} \right) \cos 2\theta + \left(\frac{\partial j_x}{\partial y} + \frac{\partial j_y}{\partial x} \right) \sin 2\theta \right) + \frac{\sqrt{3}b}{4T} \times \left(\frac{Q_{gb}}{kT} - 1 \right) \left(\frac{\partial T}{\partial x} j_x + \frac{\partial T}{\partial y} j_y \right) \right]. \quad (4)$$

The constant C_{gb} is the product $ND_0 Z^* e \delta / k$ denoting effective width of grain boundary by δ . The formulas of Eqs. (3) and (4) are applicable not only to the straight shaped line, which results in uniform current density and one-dimensional temperature distribution, but also to a complicated shaped line such as an angled line, which results in two-dimensional distributions of current density and tem-

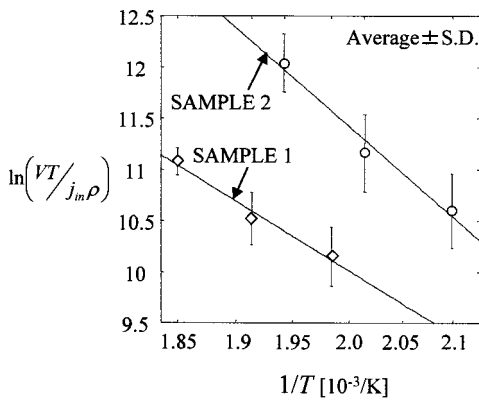


FIG. 2. The value of $\ln VT/(j_{in}\rho)$ plotted against $1/T$ for Samples 1 and 2. Activation energy Q_{gb} is given from the slope of this line, $-Q_{gb}/k$. The error bars represent standard deviation of the experimental data.

perature. The quantities j_x and j_y are the components of current density vector \mathbf{j} in Cartesian coordinates x and y . The atomic flux divergence AFD_{gen} gives the change in number of atoms per unit volume and unit time.

The distributions of the current density and temperature in the formulas are obtained by numerical analysis. The fundamental equations in the analysis are expressed as follows: Governing equation concerning electrical potential ϕ_e ;

$$\nabla^2 \phi_e = 0, \tag{5}$$

Ohm's law;

$$\mathbf{j} = -\frac{1}{\rho_0} \text{grad } \phi_e, \tag{6}$$

equation of steady-state heat conduction;¹⁰

$$\lambda \nabla^2 T + \rho_0 \mathbf{j} \cdot \mathbf{j} + (\rho_0 \alpha \mathbf{j} \cdot \mathbf{j} - H)(T - T_s) = 0, \tag{7}$$

where the resistivity in the electrical problem is assumed to be constant with sufficient approximation, λ is the thermal conductivity, H is the constant concerning the heat flow from the line to the substrate, and $\nabla^2 = \partial^2/\partial x^2 + \partial^2/\partial y^2$.

The constants concerning film characteristics are determined by the following experiment using the straight shaped line. The constants ρ_0 and α are obtained by measuring the electrical resistance of the straight metal line under low current density enough to neglect the temperature distribution. The constant H is obtained so that the electrical resistance of the metal line, which is calculated based on the temperature distribution from the finite element (FEM) analysis, equals to the measured value. The activation energy for polycrystalline line Q_{gb} is given as the slope of $\ln VT/(j_{in}\rho)$ vs $1/T$ plot shown in Fig. 2, where the variable V is the volume of void within a center region of the line after supplying current for a certain time in any three cases of the accelerating condition. The volume of void is inferred by multiplying the film thickness to total area of void measured from the scanning electron microscopic (SEM) image. Average grain size b is measured by using a focused ion beam equipment. The constants $\Delta\phi$ and C_{gb} are determined in the way described below so that the void volume calculated by using AFD_{gen} with the assumed values of $\Delta\phi$ and C_{gb} equals the experimental value. The value of $\Delta\phi$ is given by iteration method so that

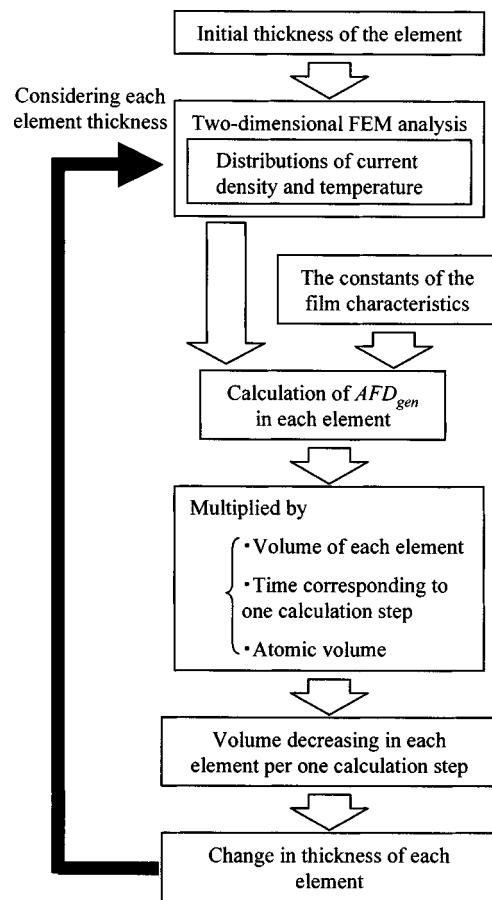


FIG. 3. Computation procedure for the numerical simulation of the processes of line failure. The thickness of the element is changed by this procedure.

the ratio of the calculated void volume within the center region of the line to that near the cathode end is the same as the ratio of the measured void. By consideration of the ratio of the void volume based on Eq. (4), the constant $\Delta\phi$ is obtained leaving the constant C_{gb} unknown. After the procedure just mentioned, only C_{gb} remains an unknown constant. The constant C_{gb} is obtained by only one relationship of void volume measured experimentally with the calculated one. Thus all unknown constants are determined from only a simple experiment using the straight line.

B. Numerical simulation using AFD_{gen}

Lifetime and failure location in the polycrystalline line are predicted by means of numerical simulation of the processes of void initiation, its growth to line failure using AFD_{gen} for a polycrystalline line, where the change in distributions of current density and temperature with void growth is taken into account on the calculation of AFD_{gen} .

In the numerical simulation the metal line is divided into elements. The smaller size of the element will give more realistic results. The thickness of the element is changed by the following procedure as shown in Fig. 3. At first, the distributions of current density and temperature in the metal line are obtained by two-dimensional FEM analysis. The di-

vergence AFD_{gen} in each element is calculated by using these distributions and the constants of the film characteristics which are determined in advance from the acceleration test. The volume decreasing in each element per one calculation step in the simulation is given by multiplying the volume of each element, the time corresponding to one calculation step, and the atomic volume to the calculated AFD_{gen} , where one calculation step is assigned to realistic time. Based on the decrement in the volume, the thickness is decreased in each element. In the element whose thickness is decreased, the void whose depth corresponds to the decrement in the thickness of the element is regarded as being formed. The FEM analysis of current density and temperature in the metal line is carried out again considering each element thickness. The calculation shown in Fig. 3 is carried out repeatedly.

Numerical simulation following this procedure is able to predict well the distribution of void after a certain time and the failure site. In order to predict the lifetime, the following consideration is required in the simulation. It is a morphology of void growth that the voids grow selectively along the grain boundary, resulting in slit-like voids extending toward linewidth and linking each other. Although the parameter AFD_{gen} is derived based on the assumption of void formation at the grain boundary, it is extended to the expectation of void formation at any point in the metal line. Here, configuration of the void formation is transformed to the formation of a slit-like void along the grain boundary. In the mesh generation, the exclusive elements constituting the slit-like void are allocated as shown in Fig. 4, indicating an example of the finite element model of the line used as shown later in Fig. 6. The thickness of only the element for the slit-like void is decreased based on AFD_{gen} calculated in the element and the neighboring elements, but the neighboring elements do not change in thickness. Pitch of the slit is defined as being an average grain size. The width of the slit, which is one of the film characteristic constants, is obtained following the procedure shown in Fig. 5. An acceleration test is performed until the line failure with SEM observation. From the SEM image of the metal line obtained just before the failure, the crowded region of the slit-like void, where the failure will occur soon, is extracted so as to draw the region in an outline. Dividing the length of the crowded region measured along longitudinal axis of the line by the pitch of the slit b gives the number of the slit which the crowded region would contain. On the other hand, the total area of the slit-like voids is measured within the crowded region. By dividing the total void area by the number of the slit and linewidth, an effective width of the slit in the simulation is obtained. An experiment for determining the slit width is performed by using the specimens which were used for determining the constants ρ_0 , α , H , $\Delta\phi$, Q_{gb} , and C_{gb} .

Considering the change in thickness of the exclusive elements for the slit, the calculation process of the numerical simulation for the lifetime prediction is carried out repeatedly until the metal line fails, which is defined as the state that the entire linewidth is occupied by elements whose temperature exceeds the melting point and/or elements penetrating the thickness. Here the element thickness smaller than an infinitesimal threshold value is considered to be penetrating.

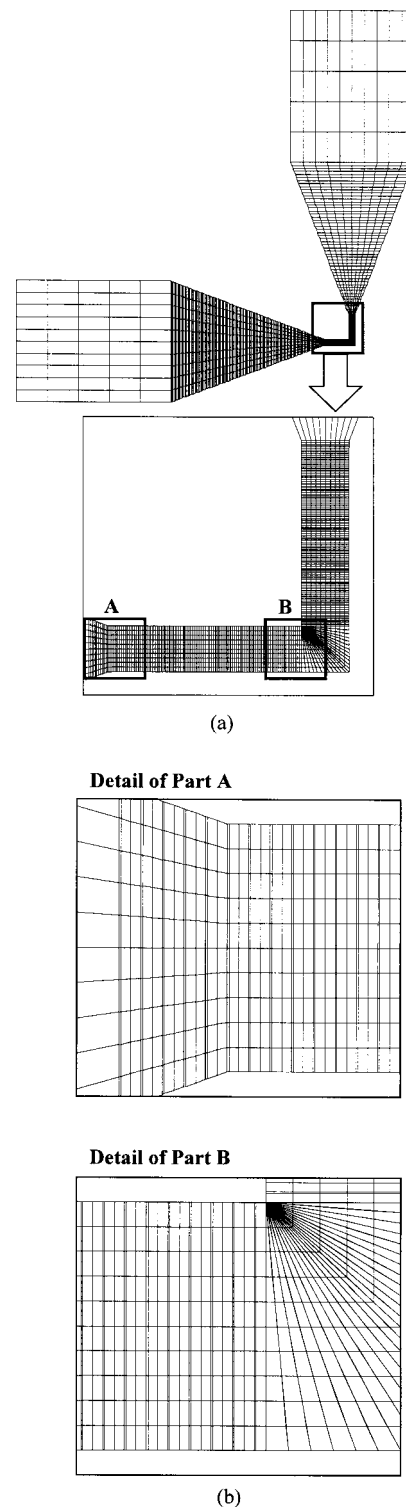


FIG. 4. (a) An example of the finite element mesh and (b) enlargement of the testing part of the specimen. The exclusive elements to constitute the slit-like void are allocated in the mesh generation. In details of (A) and (B), the element for the slit-like void is illustrated by very slim rectangle.

The threshold value is found so that the predicted lifetime is converged in the numerical simulation. The threshold value used is 2×10^{-3} times the initial film thickness. Thus the numerical simulation predicts the lifetime of the metal line under operating conditions as well as the failure site.

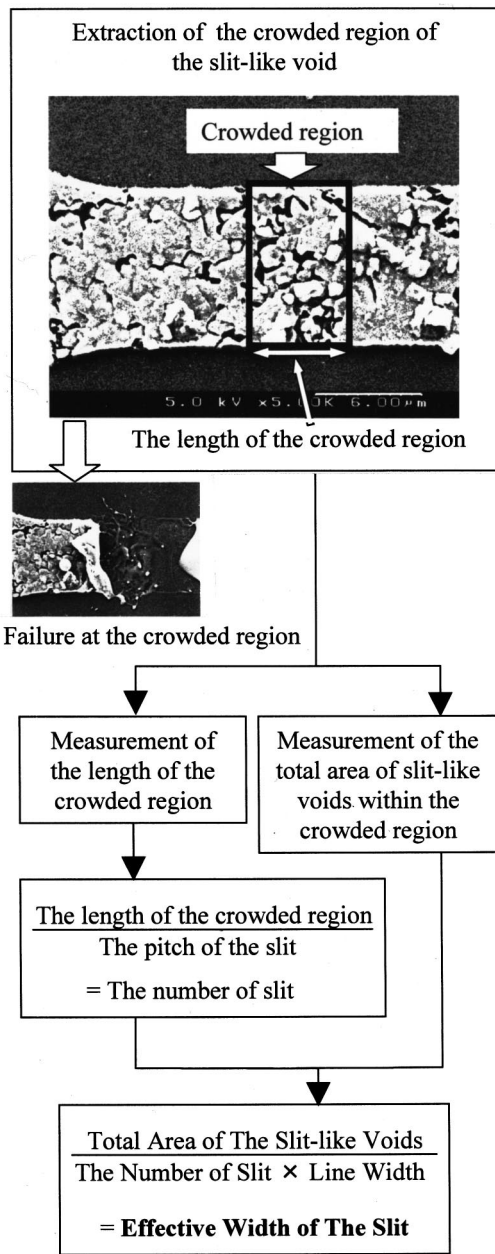


FIG. 5. Procedure to determine the effective width of the slit-like void. From the SEM image of the metal line obtained just before the failure, the crowded region of the slit-like void is extracted so as to draw the region in outline. Dividing the length of the crowded region measured along the longitudinal axis of the line by the pitch of the slit b gives the number of the slit that the crowded region would contain. On the other hand, the total area of the slit-like voids is measured within the crowded region. By dividing the total void area by the number of the slit and linewidth, an effective width of the slit to be supposed in the simulation is obtained.

III. VERIFICATION OF THE PREDICTION METHOD

A. Prediction

Two aluminum lines shown in Fig. 6 were used to predict the lifetime and the failure site. It is noted that the angled metal line results in two-dimensional distributions of current density and temperature and that all constants required for the prediction are given by the acceleration test using straight lines. Let us call the two lines Samples 1 and 2. They differ not only in dimension but also testing condi-

	A[μm]	B[μm]	Thickness [μm]	J_m [MA/cm ²]	T_s [K]
SAMPLE 1	10	40	0.56	9.0	373
SAMPLE 2	20	80	0.36	7.5	413

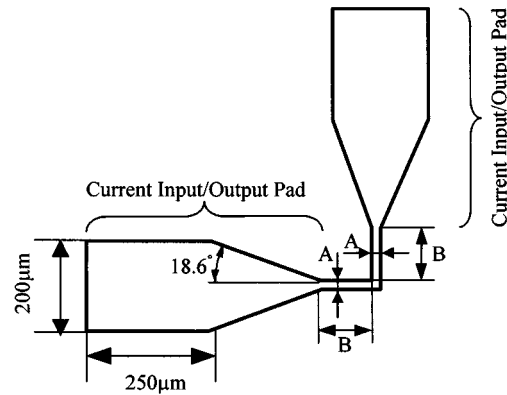


FIG. 6. Two aluminum polycrystalline lines used to predict the lifetime and the failure site. Testing conditions for the two lines, Samples 1 and 2, are also shown. The angled metal line results in two-dimensional distributions of current density and temperature.

tions as shown in Fig. 6. High current density and temperature, relative to the general operating condition, were chosen as the testing conditions to reduce the time required for the experiment of verification. The film characteristic constants to calculate AFD_{gen} were obtained by the method described in Sec. II A as shown in Table I. The values of Q_{gb} for Samples 1 and 2 were obtained from Fig. 2. By performing the numerical simulation, electromigration failure was predicted for Samples 1 and 2, respectively.

The changes in AFD_{gen} distribution and void distribution with time in the case of Sample 1 are shown in Figs. 7 and 8, respectively, and the changes in distributions of AFD_{gen} and void in the case of Sample 2 are shown in Figs. 9 and 10, respectively. The change in void distribution with time is indicated by contour line of the film thickness. The distribution of AFD_{gen} varies with time because of the changes in distributions of current density and temperature with the void growth. In the case of Sample 1, the metal line failure was predicted to occur with 7500 s in lifetime and at the cathode

TABLE I. Constants used in simulation.

	Sample 1	Sample 2
$\rho_0(\Omega \mu\text{m})$	4.45×10^{-2} (at 373 K)	4.95×10^{-2} (at 413 K)
α (/K)	0.003 20 (at 373 K)	0.00284 (at 413 K)
b (μm)	0.8	0.8
Q_{gb} (eV)	0.5668	0.8099
$\Delta\phi$ (deg)	-0.8	-5.3
C_{gb} (KC/J s)	-1.07×10^{18}	-1.07×10^{20}
λ [W/($\mu\text{m K}$)] ^a	2.33×10^{-4}	2.33×10^{-4}
H [W/($\mu\text{m}^2 \text{K}$)]	5.6×10^{-6}	5.3×10^{-6}
effective width of slit (μm)	0.060	0.065

^aSee Ref. 11.

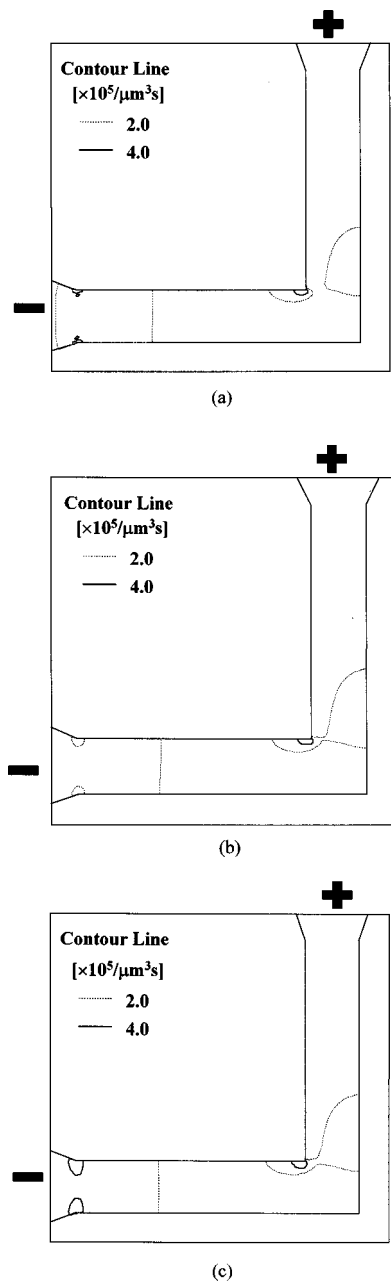


FIG. 7. Change in AFD_{gen} distribution with time in the case of Sample 1: (a) 0 s, (b) 4000 s, and (c) 6000 s.

end at the failure location. On the other hand, the failure was predicted for Sample 2 to happen with 3500 s in lifetime and at the cathode side of the corner at the failure location.

B. Experiment

In order to verify the results of the prediction, an experiment was performed concerning the same line dimension and under the condition as those in the simulation. Eleven specimens were used for Sample 1 and 12 were used for Sample 2. Aluminum film was deposited by vacuum evaporation on a silicon substrate which was covered with silicon oxide. The specimens were patterned by etching after annealing. The experiment was performed using a setup shown in Fig. 11 and the specimen was observed by SEM after the metal line becomes open.

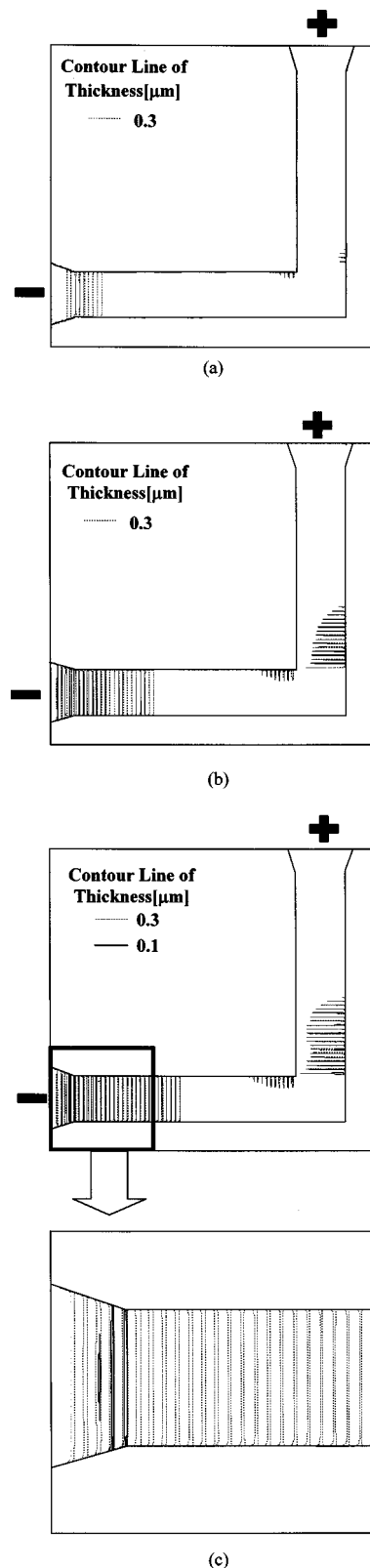


FIG. 8. Change in void distribution with time indicated by contour line of the film thickness in the case of Sample 1: (a) 4000 s, (b) 6000 s, and (c) 7500 s.

Figures 12 and 13 show the experimental results with frequency distribution of the failure site in the line and the mean-time-to-failure. In the case of Sample 1, the mean-time-to-failure obtained from all 11 specimens was 6731 s

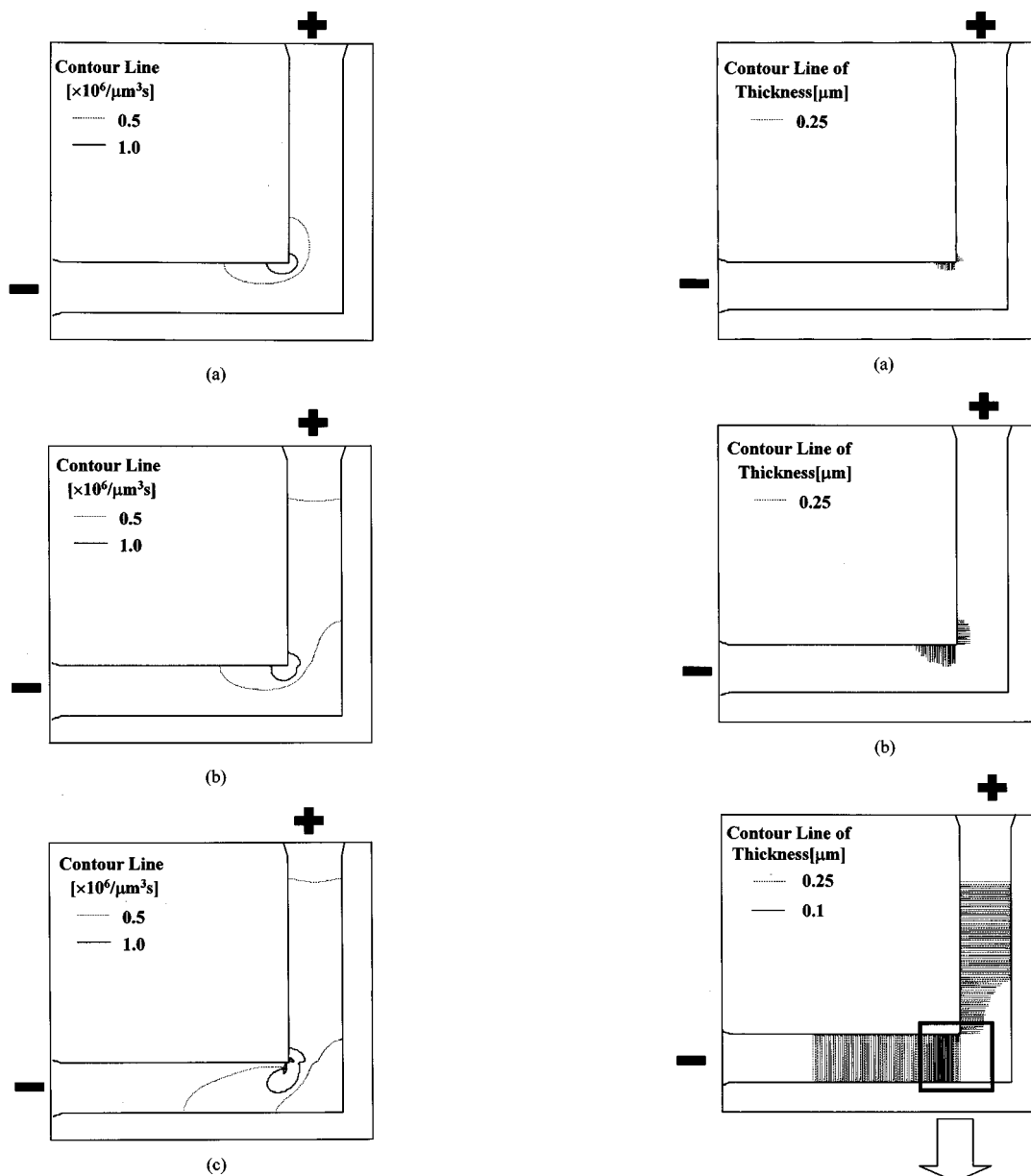


FIG. 9. Change in AFD_{gen} distribution with time in the case of Sample 2: (a) 0 s, (b) 1500 s, and (c) 2500 s.

and the most frequent failure site was cathode end of the line. The mean-time-to-failure from six specimens which opened at the predicted failure site, that is, the cathode end was 6820 s, and it was close to the mean-time-to-failure from 11 specimens. On the other hand, the mean-time-to-failure obtained from all 12 specimens was 3655 s and the cathode side of corner was one of the most frequent sites for Sample 2. The mean-time-to-failure from four specimens which opened at the predicted failure site, that is the cathode side of the corner, was 4095 s and it was close to the mean-time-to-failure from 12 specimens.

Good agreement between the prediction and the experimental result was obtained in the lifetime and the failure location. Although the failure site in the experiment somewhat spread, the most frequent site was predicted both in Samples 1 and 2. The second most frequent site in Sample 1 and the other most frequent site in Sample 2 corresponded to

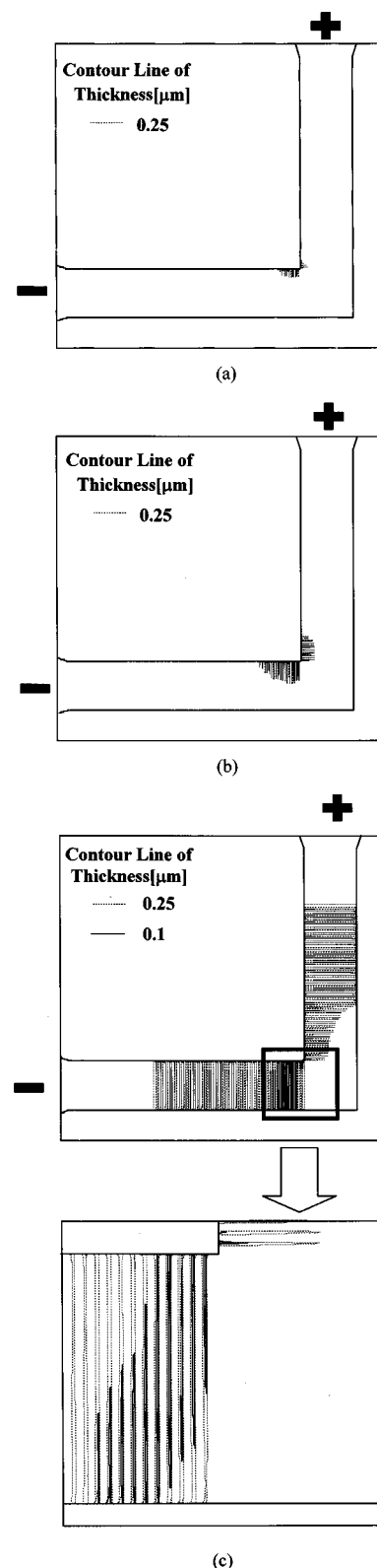


FIG. 10. Change in void distribution with time indicated by contour line of the film thickness in the case of Sample 2: (a) 1500 s, (b) 2500 s, and (c) 3500 s.

the notable region of the void formation predicted in the simulation. From this it was shown that once the film characteristics and operation condition were given, the lifetime and the failure location of the metal line with any shape

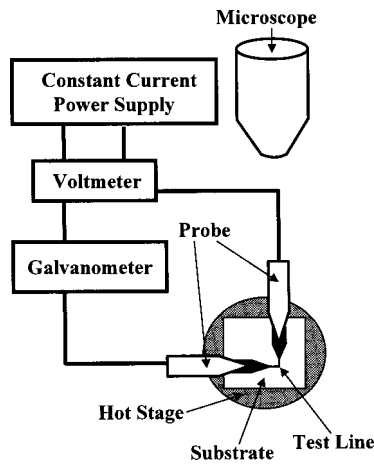


FIG. 11. Experimental setup. Test line is kept at a fixed temperature on the hot stage and subjected to dc current flow using the constant current power supply through the voltmeter, galvanometer, and probes.

under arbitrary condition were able to be predicted by means of the numerical simulation using the governing parameter of void formation due to electromigration, AFD_{gen} .

IV. CONCLUSIONS

The void formation induced by electromigration depends on the current density, temperature, their gradients, and the material characteristics such as the electrical resistivity, av -

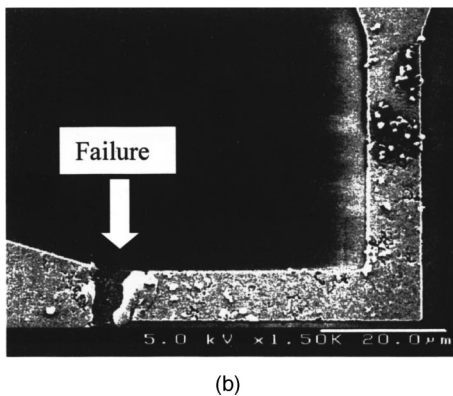
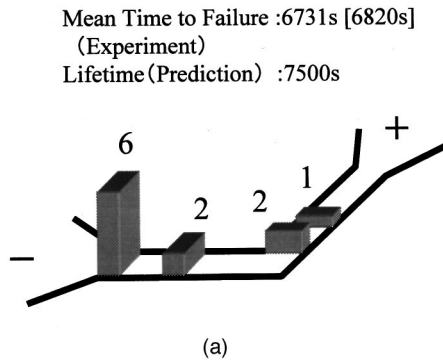


FIG. 12. Experimental results of Sample 1: (a) frequency distribution of failure site, where the mean-time-to-failure (experiment) without square brackets was obtained from 11 specimens and that in brackets was obtained from six specimens which failed at the cathode side end, and (b) an example of SEM observation of failure location.

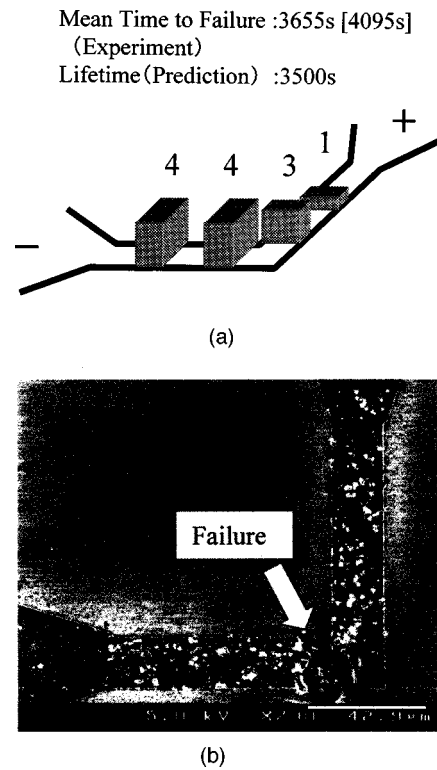


FIG. 13. Experimental results of Sample 2: (a) frequency distribution of failure site, where the mean-time-to-failure (experiment) without square brackets was obtained from 12 specimens and that in brackets was obtained from four specimens which failed at the cathode side of the corner, and (b) an example of SEM observation of failure location.

erage grain size, activation energy, relative angle between the grain boundaries, the atomic density, the diffusion coefficient, effective charge, and effective width of grain boundary. A parameter AFD_{gen} derived as a function of these factors governs the void formation. The failure of the metal line occurs as a result of void formation and its growth. The failure site is changed by the combination of factors determined by the line shape and the operating condition such as substrate temperature and input current density, that is the failure occurs at the corner of angled metal line in some cases, and occurs at the cathode end of the angled line in other cases. The present simulation based on AFD_{gen} accurately predicted the lifetime as well as the failure location of the metal line.

ACKNOWLEDGMENTS

This work was partly supported by the Ministry of Education, Science, Sports and Culture under a Grant-in-Aid for Encouragement of Young Scientists, Grant No. 10750058 and Grant-in-Aid for Scientific Research (B)(2) Grant No. 10555024. A part of this work was performed at Venture Business Laboratory in Tohoku University.

¹J. R. Black, Proc. IEEE **57**, 1587 (1969).
²S. Kondo and K. Hinode, Appl. Phys. Lett. **67**, 1606 (1995).
³M. J. Attardo and R. Rosenberg, J. Appl. Phys. **41**, 2381 (1970).

- ⁴I. A. Blech and E. S. Meieran, *Appl. Phys. Lett.* **18**, 263 (1967).
- ⁵K. Sasagawa, N. Nakamura, M. Saka, and H. Abé, *Trans. ASME, J. Elect. Pack.* **120**, 360 (1998).
- ⁶J. R. Lloyd, M. Shatzkes, and D. C. Challener, *Proceedings of the IEEE International Reliability Physics Symposium*, 1988, p. 216.
- ⁷P. B. Ghatge, *Solid State Technol.* **26**, 113 (1983).
- ⁸J. W. McPherson, *Proceedings of the IEEE International Reliability Physics Symposium*, 1986, p. 12.
- ⁹H. B. Huntington and A. R. Grone, *J. Phys. Chem. Solids* **20**, 76 (1961).
- ¹⁰R. Kirchheim and U. Kaeber, *J. Appl. Phys.* **70**, 172 (1991).
- ¹¹L. F. Mondolfo, *Aluminum Alloys: Structure and Properties* (Butterworths, London, 1976), p. 59.